Journal of The Electrochemical Society, **164** (2) F22-F31 (2017)
0013-4651/2017/164(2)/F22/10/$33.00 © The Electrochemical Society

Pt Electrocatalysts Supported on Functionalized Carbonaceous Materials

Natalia S. Veizaga,[z] Virginia I. Rodriguez, and Sergio R. de Miguel

Instituto de Investigaciones en Catálisis y Petroquímica "Ing. José Miguel Parera" (INCAPE), Facultad de Ingeniería Química (UNL)-CONICET., 3000 Santa Fe, Argentina

Monometallic Pt catalysts (17%wt) were prepared over Vulcan carbon (VC) and multiwall carbon nanotubes (NT). These supports were functionalized with citric or nitric acid. The characteristics of the different functionalized and non-functionalized supports were analyzed to determine the influence of the functional groups over the electrocatalytic behavior of the Pt monometallic catalyst. The functionalization treatment with nitric acid increases the concentration of strong and weak functional groups, whereas citric acid promotes the formation of acid groups with intermediate acidic strength. Catalysts prepared by conventional impregnation (CI) and supported on functionalized VC and NT display much higher electrochemical active areas than those supported on the corresponding non-functionalized carbons. Both the decrease of the metallic particle sizes and the changes in the metal-support interaction due to the presence of the functional groups would lead to a better electrochemical behavior.

Manuscript submitted August 31, 2016; revised manuscript received November 18, 2016. Published December 5, 2016.

It is a fact well acknowledged that a good electrocatalytic support should have 1) good electrical conductivity, 2) good metal-support interaction, 3) large surface area, 4) a mesoporous structure that permits the polymeric electrolyte to transport catalytic nanoparticles near the reagents, 5) good water handling capability to avoid flooding, 6) corrosion resistance, 7) easy recovery.[1] Besides, functional groups on the support surface could be CO-poisoning resistant and they could act as anchoring sites for the metallic precursor thus increasing the metal-support electron transfer that takes place during the electrochemical reaction.[2]

CO electrooxidation is possible only if the Pt-OH_{ads} is formed over the Pt catalyst, the required potential being of about 0.62 V at 25°C:[3–7]

$$Pt + H_2O \rightarrow Pt - OH_{ads} + H^+ + e^- \quad [1]$$

The electrooxidation of CO_{ads} can be described as:

$$Pt\text{-}CO + Pt\text{-}OH_{ads} \rightarrow 2Pt + CO_2 + H^+ + e^- \quad [2]$$

CO molecules can be removed by electrooxidation to CO_2 by oxygen-containing species (H_2O) as OH_{ads}. Nevertheless this reaction is highly inhibited in the Pt surface due to the competence between CO and H_2O adsorptions.[8]

Electrocatalysts were dispersed as nanoparticles over a carbonaceous support surface that has the proper electrical conductivity to act as electrode, so as to decrease the Pt loading. Vulcan carbon is the most ordinary support but mesoporous carbon, carbon nanofibers or nanotubes can also be used, for they have largely showed better electrochemical properties than the former. Nanotubes are graphene layers cylindrically rolled with high aspect ratio, low density and high surface area, these characteristics giving good mechanical strength with an open porous structure that improves its stability during the cell operation.[9]

Latest studies about the use of NT as electrocatalyst supports try to optimize the surface chemistry in order to improve the metal-support interaction. Carbon nanotubes have few oxygen functional groups over the surface and its surface chemistry can be modified by oxidation treatments both in liquid or gas phase in order to create functional groups.[10–12] The different functional groups not only modify the electrocatalyst performance but the acid-base and redox properties as well even though their effect on the Pt anchorage and dispersion is still being discussed. Some authors think the oxygen surface groups lead to a good Pt dispersion[13,14] but for other they have no or negative influence over the active phase dispersion.[15]

Research has showed that it is the surface chemistry of the support that influences the catalyst performance. Since the carbon surface is not inert, during the electrochemical reaction, the metal-support interaction depends on platinum-support electronic effects, this involving electronic transfer from Pt clusters to surface oxygen atoms[16] that could improve the catalytic properties and the electrocatalyst stability. It is important to note that functionalization treatments also reduce the electric conductivity so further study should be done to analyze these contrasting effects.

As it was previously mentioned the surface chemistry of the carbons can be modified for example by reaction with oxidizing gases such as ozone, oxygen, nitrous oxide, nitric oxide, carbon dioxide or oxidizing solutions as nitric acid, sodium hypochlorite, or hydrogen peroxide that create functional groups with O, N or S,[17,18] these being weak acids like lactones, phenols, and carbonyl groups or strong acids like carboxyl and anhydride ones.[19,20] Oxygen surface groups are said to decrease carbon hydrophobicity and make its surface more accessible to metallic precursors during impregnation.[21] Besides, these groups modify the pH of the slurries highly influencing the impregnation. They also behave as nucleation centers that form well-dispersed metallic crystallites.

The objective of this work is focused on the study of the characteristics of the supports either functionalized or non-functionalized so as to analyze the influence of the induced surface groups on the electrocatalytic behavior of monometallic Pt catalysts.

Experimental

Preparation and characterization of the supports.—Vulcan carbon XC-72 (VC) and multiwall carbon nanotubes (NT) were used as supports. Vulcan carbon XC-72 has a specific surface area (S_{BET}) of 240 m^2g^{-1}, a pore volume (V_{pore}) of 0.31 cm^3g^{-1} and a mean particle size of 40 nm. The physical properties of the commercial multiwall carbon nanotubes (Sunnano, purity > 90%, diameter: 10–30 nm, length: 1–10 μm) are S_{BET} = 211 m^2g^{-1} and V_{pore} = 0.46 cm^3g^{-1}.

Support treatments.—NT were purified (elimination of inorganic impurities) by successive treatments with aqueous solutions (10%wt) of HCl, HNO_3, and HF, respectively, at 25°C during 48 h. After HCl and HNO_3 treatments, NT were repeatedly washed with deionized water up to a final pH = 4. After HF treatment, NT were washed with deionized water up to the final pH of this water and then dried at 120°C during 24 h. In order to eliminate sulfur compounds, a thermal treatment under hydrogen flow (5 mL H_2 $min^{-1}g^{-1}$) at 850°C during 4 h was performed.[22,23]

Since VC impurities were almost negligible, it was not necessary to purify this support.

[z]E-mail: nveizaga@fiq.unl.edu.ar

Functionalization with citric acid and HNO_3.—The functionalization of the carbonaceous supports with citric acid was carried out following the technique previously reported.[24] In this sense, a dispersion of 10 g of carbon, 10 g of citric acid (Sigma Aldrich, ACS reagent 99–102%) and 100 mL of distilled water was prepared by ultrasonic mixing for 15 min. The mixture was evaporated until a paste was obtained. This paste was dried at 120°C during 24 h, and then calcined under flowing N_2 at 300°C for 30 min. Finally, the support was crushed to a powder.

The functionalization with nitric acid was done with a technique previously reported.[21] Samples were treated with concentrated nitric acid (Sigma Aldrich, 65%) for 8 h in a condensation round bottom flask by heating up to boiling temperature (about 94–96°C). A 30 mL g^{-1} solution/carbon mass ratio was used. Then, the support was filtered and washed with distilled deionized water up to water pH. Finally, it was dried in stove at 110°C overnight.

Impurity analysis.—The analysis of the impurities was carried out by EDX on the ashes of the carbons, which were obtained by total burn-off of carbons with air at 700°C in an electric furnace.

Textural properties.—The characterization of the porous structure of the carbons was carried out by physical adsorption of N_2 at −196°C by using a Quantachrome Corporation NOVA-1000 equipment. Samples were previously outgassed at 130°C.[25]

Isoelectric point.—Isoelectric points (IP) of VC and NT were determined by titration or neutralization at constant pH in aqueous solution of KNO_3.[26,27] In order to eliminate the influence of atmospheric CO_2, the experiment was carried out under nitrogen atmosphere. Thus, the aqueous solution of KNO_3 (0.1N) was stirred, and purificated N_2 was bubbled through the system at room temperature. The pH of the solution was kept constant (pH = 7) by using HNO_3 or KOH solutions. Then, the samples (500 mg) were suspended into the aqueous solution and allowed to equilibrate, in order to obtain the corresponding IP value.

Surface chemistry.—Temperature-programmed desorption (TPD) technique was used to determine the surface chemistry of carbons. Experiments were carried out in a differential flow reactor coupled to a thermal conductivity detector. First, the sample was stabilized with He at room temperature for 1 h, and then, it was heated in He flow (9 mL min^{-1}). at 6°C min^{-1} from 25 to 750°C.

Temperature programmed reduction (TPR).—Temperature programmed reduction (TPR) measurements were carried out by using a H_2 (5%v/v)/N_2 mixture (60 mL min^{-1}) and a heating rate of 6°C min^{-1} from 25°C up to 800°C. The exit of the reactor was connected to a thermal conductivity detector.

Preparation and characterization of catalysts.—*Catalyst preparation.*—Monometallic Pt (17%wt) catalysts were prepared over non-functionalized and citric or nitric acid functionalized carbons as it was above mentioned. The preparation techniques were a deposition-reduction method in liquid phase with 0.4 M sodium borohydride (BR) as a reducing agent, and conventional impregnation (CI) followed by a thermal reduction with H_2 at 230°C for 2 h. The concentration of the reducing agent was chosen taken into account previous results.[28]

Test reactions of benzene hydrogenation and cyclohexane dehydrogenation.—Catalytic activity for benzene (Bz) hydrogenation reaction and cyclohexane (CH) dehydrogenation was determined in a differential flow reactor. Bz hydrogenation was carried out at 110°C, using a H_2/Bz molar ratio of 26 and a volumetric rate of 600 mL min^{-1}. Reaction conditions for CH dehydrogenation were: temperature = 270°C, H_2/CH molar ratio = 26 and volumetric flow = 600 mL min^{-1}. The weight of the sample was such as to obtain a conversion lower than 5%. The effluent of the reactor was analyzed by gas chromatography. Only for CH dehydrogenation, catalysts were previously reduced "in situ" in flowing H_2 at 270°C for 2 h.

Table I. Carbon nanotubes impurities before and after purification treatment.

Carbon nanotubes impurities	NT* (%wt)	NT (%wt)
Fe	2.78	0.21
Al	2.02	0.01
Cl	0.86	0.23
Si	0.34	0.01
S	0.10	0.01
Ca	0.05	0.01
Total	6.15	0.48

Transmission electron microscopy (TEM).—The surface morphology of Pt particles on VC and NT was studied via TEM (JEOL 100CX), operated at 100 kV, and magnification ranges of 80,000× and 100,000×. For each sample, a very important number of Pt particles (approximately 200) was observed.

CO stripping.—Catalysts were characterized by CO stripping in a conventional half-cell with three electrodes using a potentiostat (TEQ-02). Pure CO was bubbled in an electrolytic 0.5 M H_2SO_4 solution for 1 h and the potential was maintained constant at 200 mV. Then, N_2 was passed through to eliminate the dissolved CO.

The specific electrochemical active surface (EASS) -Eq. 3- is obtained from CO voltammetry according to:

$$EASS = \frac{(Q_{CO}/q^{S}_{CO})}{m_{Pt}} \quad [3]$$

where m_{Pt} is the Pt mass, Q_{CO} is the charge required for the oxidation of the monolayer of CO adsorbed on active sites, and q^{s}_{CO} is a reference value equal to 0.42 mC cm^{-2}.[29]

Results and Discussion

Support characterization.—It is known that the support influences the catalyst activity, this effect being explained by two facts: first, an electronic effect of the support over metallic particles that could affect the active sites over the catalyst surface and second, a geometric effect that could modify the form of the catalyst particles and in this way the activity and the number of the active catalytic sites could be changed.[30]

Two carbonaceous materials were used in this work: Vulcan carbon (VC) and multiwall carbon nanotubes (NT). Since EDAX analysis showed that NT have a high inorganic impurity content (6.15%wt), mainly Fe and Al that come from its synthesis, it was necessary to purify these NT by acid and thermal treatments, the last one being done with H_2 at 850°C for 4 h. Table I shows NT impurities before and after purification treatments. It can be seen that the impurity content decreased from 6.25% up to 0.45%. The purified NT was called NT and the raw ones, NT*.

As VC impurities were very low, it was not necessary to purify this support. The total inorganic impurity content of this support was 0.45% (0.01% Fe, 0.01% Al, 0.07% Si, 0.25% S, 0.05% Ca, 0.01% Mg, 0.05% Zn), and the sulfur content was negligible against Pt load (17%wt).

Table II shows specific surface (S_{BET}), pore volume (V_{pore}) and isoelectric point (IP) values of both supports. Isoelectric point gives an idea of acid or basic characteristics of the functionalized and non-functionalized carbonaceous materials. Different functionalization treatments were used to produce supports with different surface chemistry, i.e. different oxygenated surface groups that could affect both metallic phase deposition and the final characteristics of catalysts.

As it can be seen from Table II, the specific surface of both NT* and NT shows a slight modification. The nitric acid functionalization does not decrease the specific surface in an important way whereas

Table II. Surface area (S_{BET}), pore volumen (V_{pore}) and isoelectric point (IP) values of functionalized and non-functionalized carbons.

Support	S_{BET} (m^2g^{-1})	V_{pore} (cm^3g^{-1})	IP
Vulcan carbon (VC)	240	0.31	7.40
VC-citric acid	87	0.19	4.52
VC-HNO_3	192	0.22	3.00
Carbon nanotubes (NT*)	211	0.46	4.60
NT	198	0.42	7.00
NT-citric acid	102	0.26	5.64
NT-HNO_3	214	0.43	4.50

(NT*: unpurified carbon nanotubes).

citric acid one highly decreases it. Solhy et al.[31] reported two kinetic regimes for HNO_3 oxygenated carbon nanotubes associated to a fast formation of carboxylic groups at reaction times lower than 1 h, and with a much slower functionalization rate after 1 h. The first step is related with the consumption of amorphous carbon present on NT defects rather than to a direct attack on a graphene layer. The second step is related with a change in their intrinsic morphology due to partial destruction or diminution of the micropore wall, number of walls and closed tips, the latter being produced by blocking of the NT diameter with Fe particles. Thus, the partial destruction of micropore walls and number of walls would contribute to the decrease of the surface area, while the opening of NT tips would contribute to increase it. From these opposite effects it can be seen that the values of the textural properties of NT-HNO_3 remained practically unchanged with respect to those of NT. These effects could also explain S_{BET} and pore volume decreases of the support functionalized with citric acid. In this case, the lower specific surface could be due to the partial destruction of the pore walls (as it happens with nitric acid) and the inability of the citric acid (weaker than nitric one) to open nanotube ends and thus increase the specific surface.

The pore volume and specific surface decrease of the VC functionalized with nitric and citric acids agree with previous results from different authors[32,33] and it can be explained by the collapse of pore walls caused by concentrated acid attack.

By determining the isoelectric point (IP) of each support, impregnating conditions can be chosen, viz, impregnating solution pH, type of metal precursor (anionic or cationic). From Table II, it can be observed that both NT and VC having low concentration of acid groups (as TPD characterization corroborates) show an almost neutral pH (between 7 and 7.4), this fact being attributed to the removal of acid oxygenated groups from the support and a consequent increase in basicity due to defects in structure and/or higher exposure of the π sites that act as electron donors.[34] The IP of both supports decreases after citric acid functionalization (see Table II), this being more pronounced when functionalized with nitric acid, a stronger oxidant.

Chloroplatinic acid, H_2PtCl_6, an anionic metal precursor and strong acid was used in aqueous solution to prepare the catalysts, and it has a very low pH (1.2), lower than IPs of both functionalized supports. In consequence, a good deposition and metal-carbon support interaction can be achieved.

Figure 1 shows the amounts of acid or basic solution added versus the pH for different supports after the isoelectric point has been determined. It can be observed that VC and NT supports show amphoteric behavior. In this sense there is a wide range where the supports can adsorb both anions and cations depending on if the pH of the impregnating solution is lower than 3 or higher than 8. Hence, the $PtCl_6^{-2}$ adsorption could become significant at pH lower than 3 for all the supports in spite of the different isoelectric points.[35]

Oxidized surface groups were characterized by TPD tests. Figures 2a and 2b shows temperature programmed desorption profiles of the non-functionalized supports and nitric and citric acids functionalized ones. The profiles of non-functionalized and purified supports show a very low concentration (or absence) of surface groups.

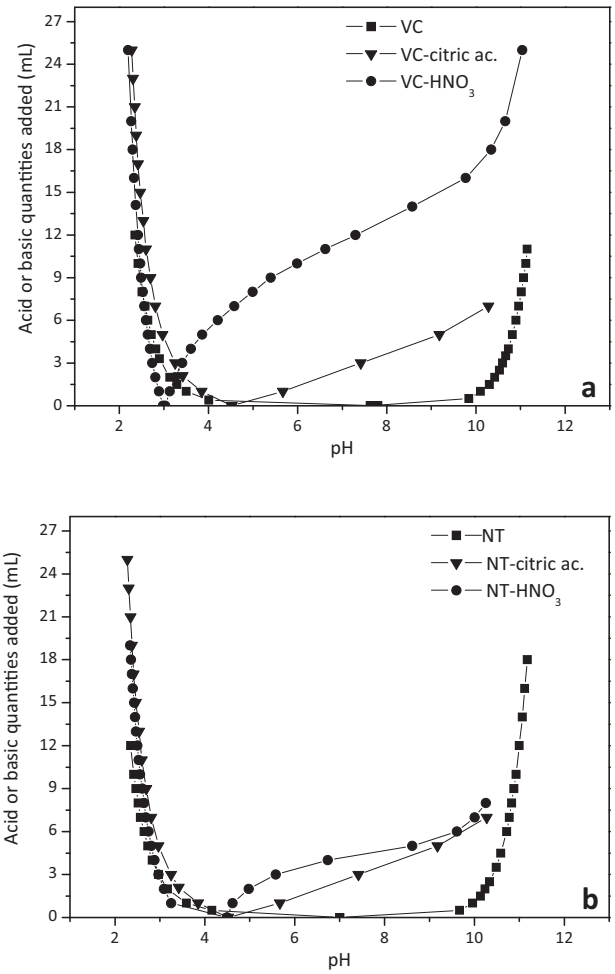

Figure 1. Amounts of acid or basic solution adsorbed versus pH. a) on functionalized and non-functionalized VC, b) on functionalized and non-functionalized NT.

When comparing IP results (Table II) with TPD profiles (Figure 2) of non-functionalized supports, it can be observed that both VC and purified NT do not show functional groups so their IPs are neutral.

It is well known that during TPD tests strong acid groups of carbonaceous materials desorb CO_2 at low temperatures (between 200 and 500°C) while weaker ones desorb CO at high temperatures (higher than 500°C).[36,37]

TPD results (Figure 2) indicate that the functionalization treatment with nitric acid gives high concentration of strongly acidic functional groups (desorbed at low temperature) and also weakly acidic ones (desorbed at high temperature) whereas citric acid promotes the formation of acid groups desorbed at intermediate temperatures (between 300 and 700°C). In this way, oxidized surface groups of different nature are produced from the functionalization treatments with both acids.

Contradictory results about the effects of oxidizing treatments have been reported in the literature. On the one hand it is said that functional groups improve the anchoring of metallic precursors and the dispersion of the metallic particles as well,[38] on the other hand the presence of surface oxidized groups lowers the metal dispersion because of the destruction of basic sites during the oxidizing treatment.[39]

Figure 3 shows TPR profiles of the different non-functionalized and functionalized with nitric and citric acids carbonaceous materials. TPR profiles of VC and purified NT without treatment do not show any hydrogen consumption, this agreeing with the lack of functional groups indicated by TPD tests (Figure 2).

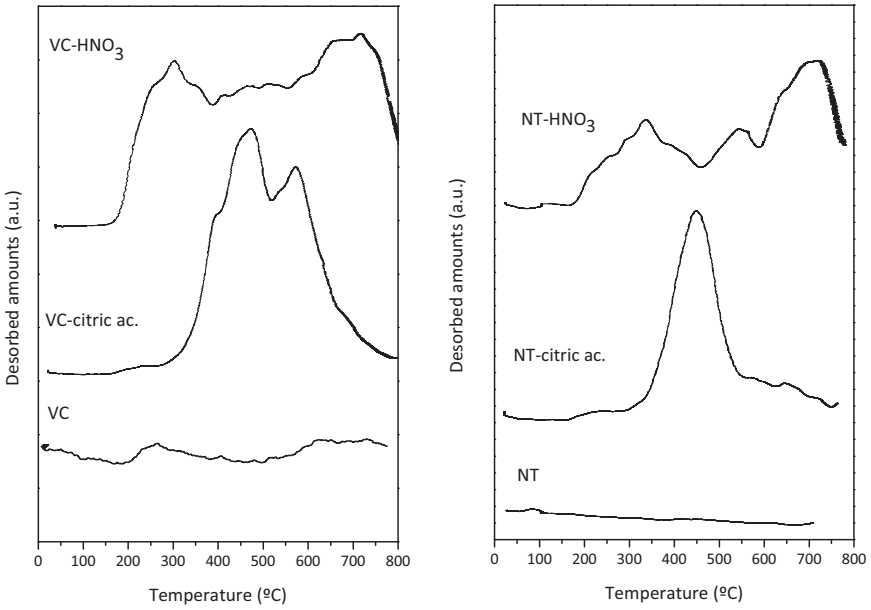

Figure 2. TPD profiles of supports functionalized with different oxidation agents and non-functionalized ones.

TPR profiles of functionalized supports show a hydrogen consumption zone mainly at high temperatures (>500°C) as Figure 3 indicates. The TPR profile of the VC-HNO_3 support has a hydrogen consumption zone that begins at about 550°C and ends at 750°C that corresponds to CO desorption at high temperatures in the TPD test. This hydrogen-consumption peak could be related to oxidized surface groups (C[O]) that release CO as some authors suggest.[40–42] The desorption of weak oxidized surface groups would produce new reactive sites (C_f) over the carbon surface that could interact with hydrogen at high temperatures as the following reactions show:

$$2C\,[O] \leftrightarrow C_f + CO \qquad [4]$$

$$C_f + H_2 \leftrightarrow C\,[H]\,, C\,[H_2] \qquad [5]$$

The same explanation could be given to hydrogen consumption zones at high temperatures observed in TPR profiles of NT-HNO_3. It is worth noticing that for VC and NT functionalized with citric acid, because of the low desorption of functional groups (Figure 2), the hydrogen consumption peak at high temperatures was smaller.

Characterization of Pt/carbon catalysts.—Figure 4 shows TPR profiles of different Pt catalysts supported on VC and NT prepared by deposition-reduction in liquid phase (RB) and compared with conventionally impregnated (CI) ones. It can be seen (Figures 4a and 4b) that liquid phase reduction of functionalized catalysts reduces Pt to metallic state so no hydrogen consumption peaks were observed in the Pt reduction zone (about 200°C). There is a wide reduction peak at high temperature (>400°C) caused by the interaction of atomic hydrogen with unsaturated reactive sites left by the desorption of functional groups of the support.[35]

For catalysts supported on non-functionalized VC and NT prepared by CI, there is a reduction peak with a maximum at about 200°C (Figures 4c and 4d) that could correspond to the reduction of Pt precursor complexes as it was mentioned in the literature for TPR of Pt catalysts supported on carbonaceous materials with different oxidizing treatments.[23,38,43,44]

The TPR profiles of catalysts supported on VC and functionalized with citric and nitric acids (Figure 4c) show a Pt reduction peak at lower temperatures (between 80–120°C) because of easily reduced Pt species. For functionalized NT (Figure 4d) it is also observed a shift

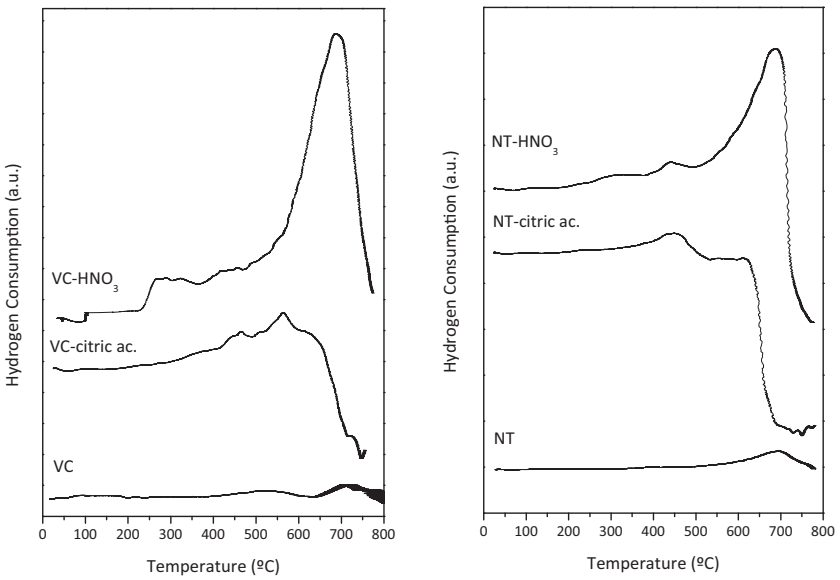

Figure 3. TPR profiles of supports functionalized with different oxidizing agents compared to the corresponding non-functionalized support.

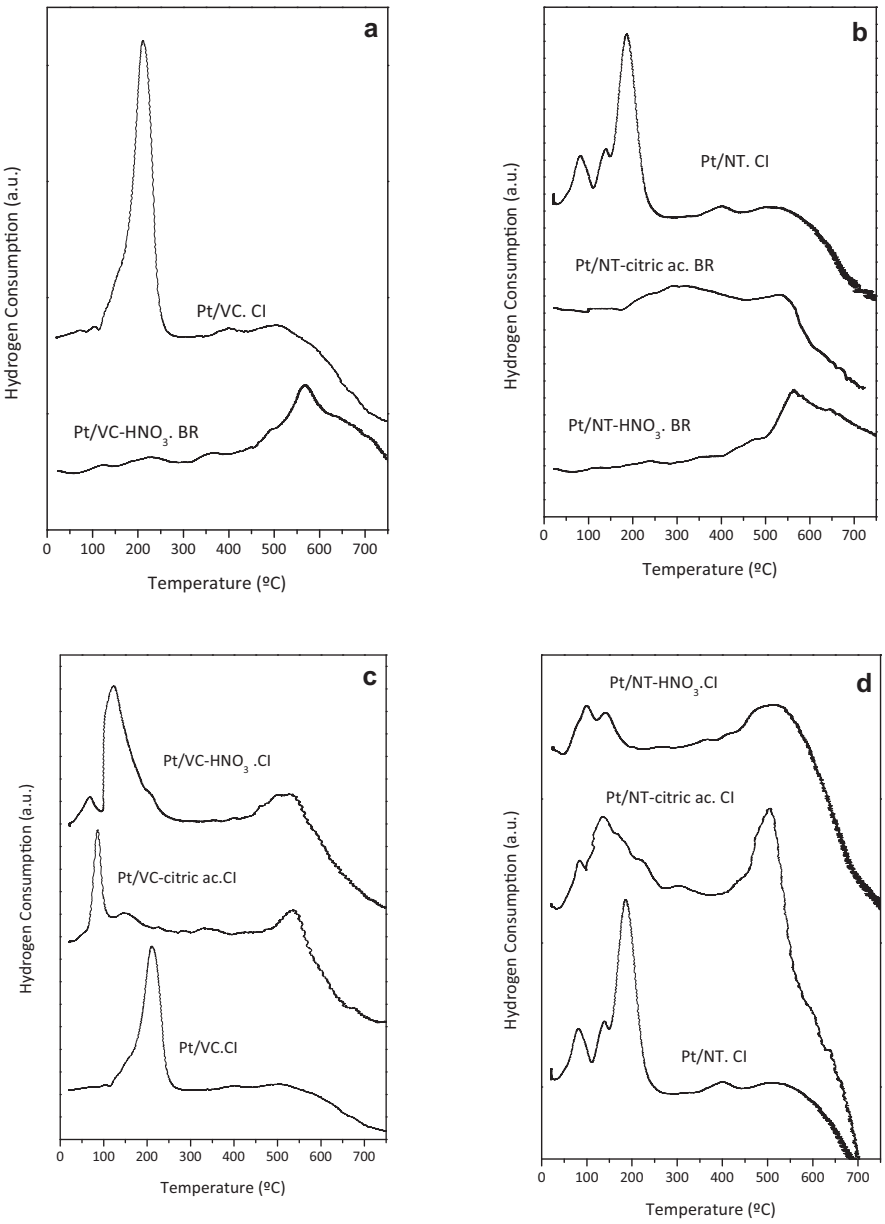

Figure 4. TPR profiles of monometallic catalysts supported on functionalized and non-functionalized carbons prepared by BR (a and b) and CI (c and d).

of the Pt peak to lower temperatures that it is not so noticeable as in the first case. It can be seen that functional groups on the support could enhance the adsorption of Pt species that are easily reduced at lower temperatures.

In catalysts supported on functionalized supports it can be observed a hydrogen consumption zone at high temperatures (>450°C) related with desorption of weak functional groups and the formation of unsaturated reactive sites that could interact with hydrogen.

In order to characterize the metallic phases of the electrocatalysts, two test reactions, benzene hydrogenation and cyclohexane dehydrogenation, were used. Both of them are structure-insensitive reactions,[45,46] which are carried out on the surface active atoms of the catalyst and involve only one exposed site. For both reactions, two parameters are important: the reaction rate, since it can be considered as an indirect measurement of exposed surface Pt atoms, and the activation energy, since its value can be modified if the nature of the metallic site is changed by some effect, such as, the presence of a second metal or the different properties of the support (electronic modification in the metal-metal or metal-support interaction).

The metallic phase of the catalysts prepared by borohydride reduction was characterized by benzene hydrogenation since this reaction is carried out at low temperatures (110°C) without producing changes in the metallic phase of the catalysts prepared by BR technique. Table III compares the values of initial activity (R^0_{Bz}) and activation energy (Ea_{Bz}) for the monometallic catalysts supported on different functionalized and non-functionalized carbons.

R^0_{Bz} values were rather constant for the different Pt catalysts prepared by BR technique, so they do not depend on the support and the type of functionalization method. The activation energy (Ea_{Bz}) values

Table III. Benzene hydrogenation test reaction (Bz) of liquid phase reduced catalysts with $NaBH_4$ 0.4 M.

Catalysts	R^0_{Bz} (mol h^{-1} g Pt^{-1})	Ea_{Bz} (Kcal mol^{-1})
Pt/VC. BR	2.6	10.1
Pt/VC-citric ac. BR	3.0	10.4
Pt/VC-HNO_3. BR	3.6	9.6
Pt/NT. BR	3.9	13.5
Pt/NT-citric ac. BR	3.4	11.8
Pt/NT-HNO_3. BR	2.6	11.2

Table IV. Initial activities and activation energies in cyclohexane dehydrogenation reaction for monometallic Pt catalysts prepared by CI.

Catalysts	R°_{CH} (mol h^{-1} g Pt^{-1})	Ea_{CH} (Kcal mol^{-1})
Pt/VC. CI	6.6	28.1
Pt/VC-citric ac. CI	0.6	*
Pt/VC-HNO_3. CI	2.9	30.8
Pt/NT. CI	5.5	21.4
Pt/NT- citric ac. CI	1.4	29.5
Pt/NT-HNO_3. CI	2.4	31.1

*not determined due to the low activity of the sample.

give an idea about modifications of the reaction active sites and in this case the values show a slight decrease of the Ea_{Bz} for functionalized NT supported catalysts (mainly for those treated with nitric acid) respect to the non-functionalized ones. These small changes would indicate a slight modification in the active site-support interaction caused by the functionalization treatment. With respect to catalysts supported on functionalized VC, the activation energies are similar to those corresponding to the catalyst supported on non-functionalized VC, thus indicating no modification of the metal-support interaction.

Conventionally impregnated (CI) catalysts were characterized by cyclohexane dehydrogenation and from Table IV it can be observed that the initial activities (R°_{CH}) of functionalized supported catalysts are lower than those of the corresponding non-functionalized sup-

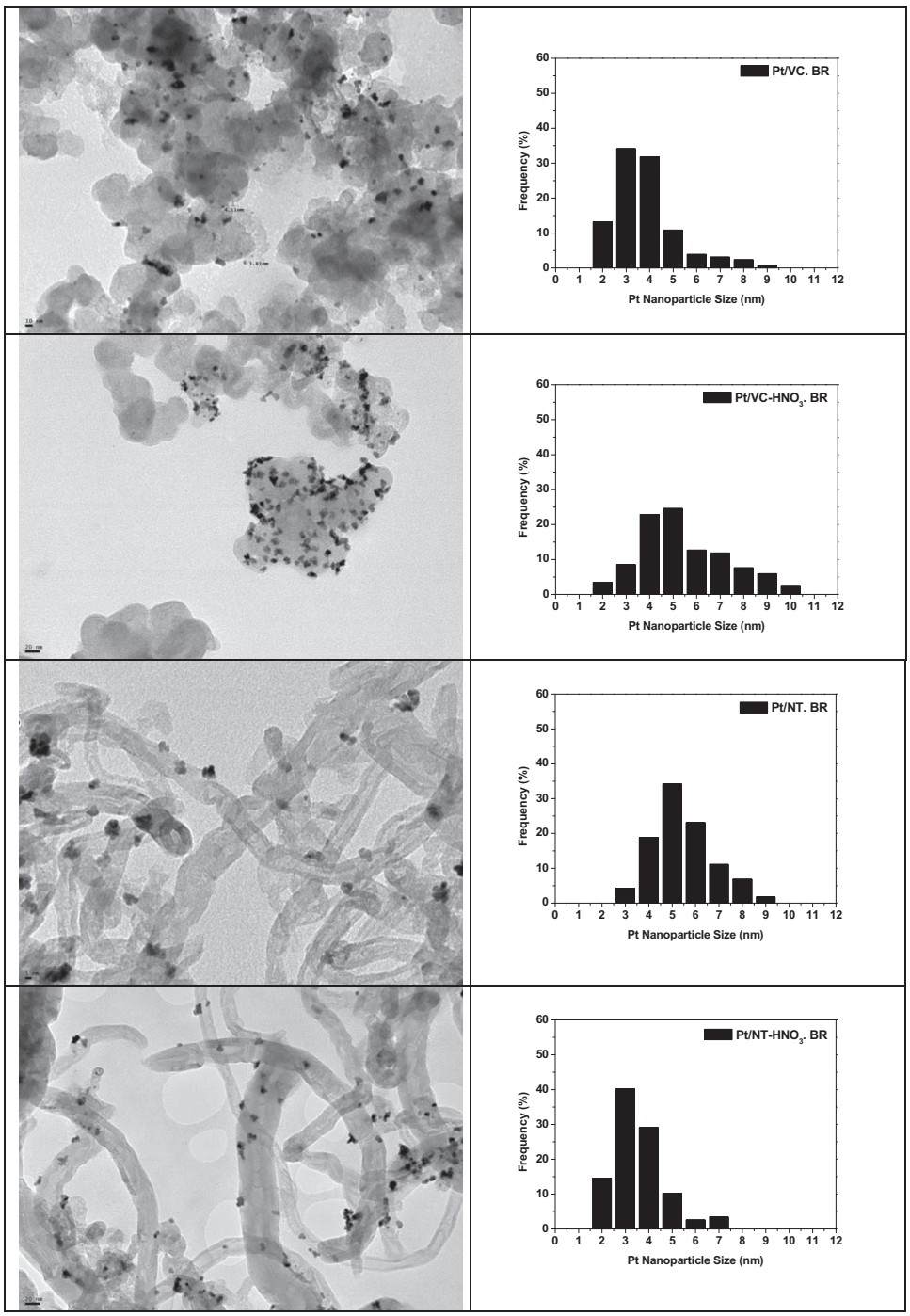

Figure 5. TEM images and corresponding size distribution histograms of: a) Pt/VC, b) Pt/VC-HNO_3, c) Pt/NT, and d) Pt/NT-HNO_3 prepared by BR.

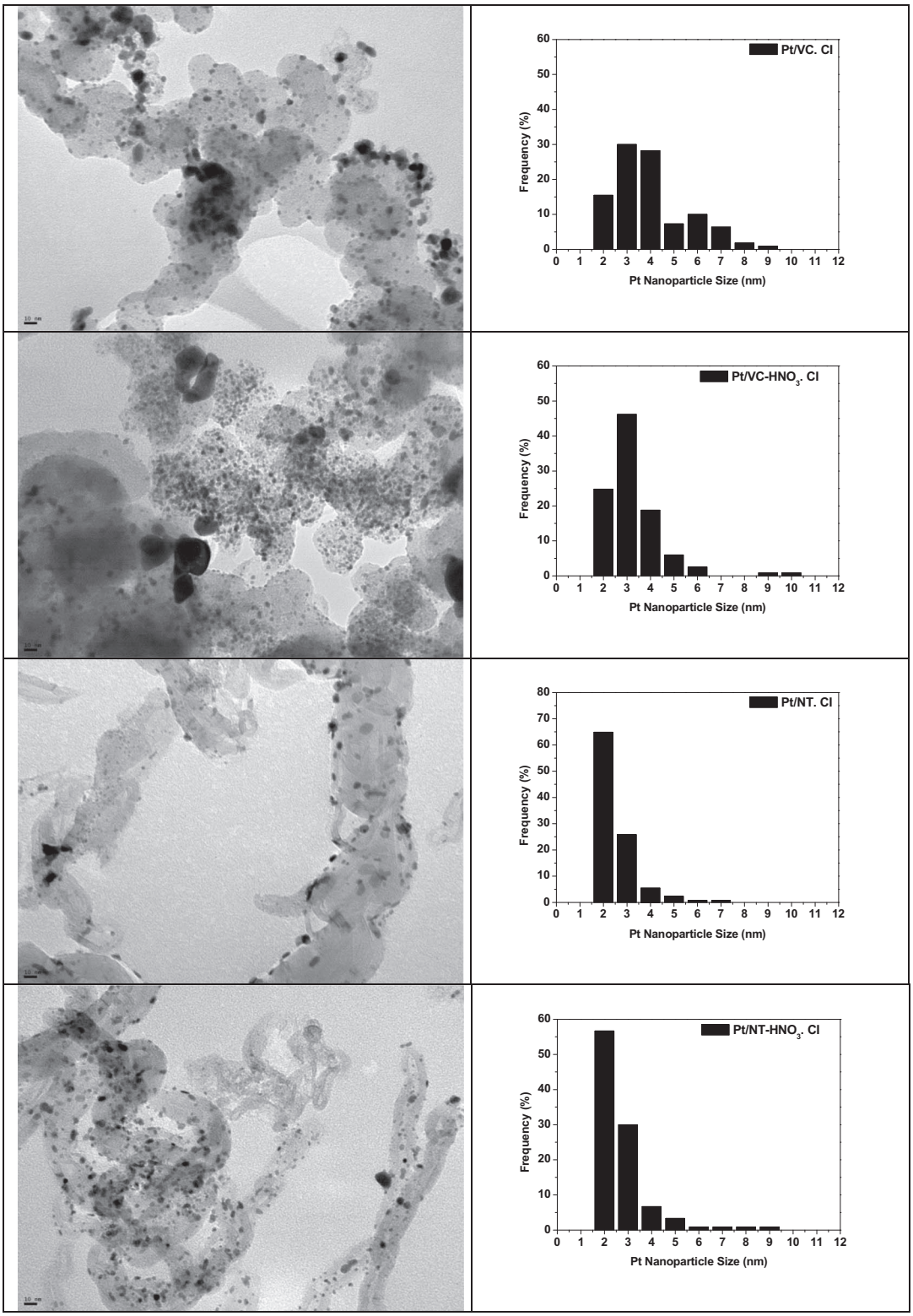

Figure 6. TEM images and their corresponding particle size distribution histograms of: a) Pt/VC, b) Pt/VC-HNO_3, Pt/NT and Pt/NT-HNO_3 prepared by CI.

ported ones, the first ones also showing a higher activation energy (Ea_{CH}), mainly for NT. This would be indicating that for impregnated catalysts, an important change in the interaction between the active metal and the support is produced, probably due to the influence of oxidized groups over the adsorption mechanism of the metallic precursor on the support.

Figures 5 and 6 present TEM results for the different Pt electrocatalysts. For each catalyst, a microphotography and the distribution of particle sizes are displayed. Besides, Table V shows the mean value of the particle size for the catalysts.

TEM results indicate that Pt catalysts supported on both supports and prepared by borohydride reduction method (BR) display mean

Table V. Mean particle size determined by TEM for monometallic Pt catalysts prepared by BR and CI.

Catalysts	d_{TEM} (nm)
Pt/VC. BR	3.6
Pt/VC-HNO_3. BR	5.0
Pt/NT. BR	5.0
Pt/NT-HNO_3. BR	3.2
Pt/VC. CI	3.5
Pt/VC-HNO_3. CI	2.8
Pt/NT. CI	2.1
Pt/NT-HNO_3. CI	2.2

particle sizes higher than the ones prepared by the impregnation (CI) method (see Table V). In this sense, the second method (CI) would assure a stronger interaction between the support and the metallic precursor during impregnation, leading to higher dispersions of the metallic phase.

In the case of catalysts prepared by BR method, only those supported on NT functionalized with HNO_3 show a decrease of the metallic particle with respect to the catalyst supported on non-functionalized NT. This fact would be in agreement with test reaction results for this catalyst, which showed a slight modification in the active site-support interaction caused by the functionalization treatment (Table III).

For catalysts prepared by CI method and supported on VC, there is a decrease of the mean particle size when the support is functionalized with HNO_3. In this case, the modification of the metal-support interaction due to the functionalization treatment, observed by test reactions, would be responsible for the deposition of the metallic precursor in the form of smaller particle sizes. For catalysts prepared by CI and supported on NT, test reaction results also show a modification of the interaction between the carbonaceous material and the metallic phase due to the functionalized support, however the metallic particle size determined by TEM (Table V) is very similar when comparing the sample supported on functionalized and on non-functionalized NT. This fact is probably due to Pt/NT catalysts have a very low mean particle size, about 2 nm.

Taking into account that CO species are the main poisoning intermediate, a good catalyst for methanol electro-oxidation should possess excellent CO electro-oxidizing ability, which can be reflected from CO stripping test. Figures 7 and 8 show CO stripping results of Pt catalysts prepared by BR and CI techniques, respectively, and supported on the non-functionalized and functionalized carbonaceous materials. From cyclic voltammetries it was possible to obtain the electrochemical areas, EASS (Tables VI and VII) and also the CO onset potential.

The catalyst prepared by BR and supported on VC functionalized with citric acid, displayed lower onset potential than that supported on VC functionalized with nitric acid and even lower than the samples on non-functionalized supports (Figure 7 and Table VI). By using NT as support, both functionalized catalysts prepared by BR showed lower onset potential than the catalysts supported on the non-functionalized support. The electrochemical areas (EASS) for the catalysts supported on functionalized carbons are higher than the ones observed for those supported on non-functionalized ones (Table VI). However, the differences observed in CO stripping between catalysts prepared by BR and supported on functionalized and non-functionalized carbons were not very important. This fact could be due to the deposition technique (BR) that would slightly modify the active site-support interaction induced by the functionalization treatment. Besides, the presence of sodium borohydride (BR) could reduce the surface oxygen groups. In fact, Zhong et al.[47] reported that hydroxyl groups were the main reduction products of carboxylic anhydrides, carbonyls, and even lactones by BR technique, whereas ether and epoxy groups remained on the NT surface. Hence, this decrease of surface oxygen groups could also influence negatively the electrochemical performance of Pt electrocatalysts prepared by deposition-reduction method in liquid phase with sodium borohydride.

For catalysts prepared by impregnation technique (CI), important differences were found from cyclic voltammograms of CO stripping. In fact, Figure 8 and EASS values in Table VII showed that functional groups developed in VC and NT by treatments with nitric or citric acid, highly increase the Pt electrochemical area. In this sense the increase of the EASS values of the catalysts supported on functionalized carbons are between 4 and 6 times higher than those of the corresponding catalyst supported on the non-functionalized carbonaceous material (see Table VII). Moreover, functional groups in these catalysts favor CO oxidation at lower potentials mainly in catalysts supported on VC, since CO oxidation in Pt/VC. CI catalyst begins at 500 mV vs. Ag/AgCl and the onset potential begins at 435 mV vs. Ag/AgCl for Pt/VC-citric acid. CI catalyst and 480 mV for Pt/VC-HNO_3 one (see Table VII). However, for catalysts supported on NT, the onset values ($\cong$ 450 mV) were very similar both for functionalized and non-functionalized nanotubes.

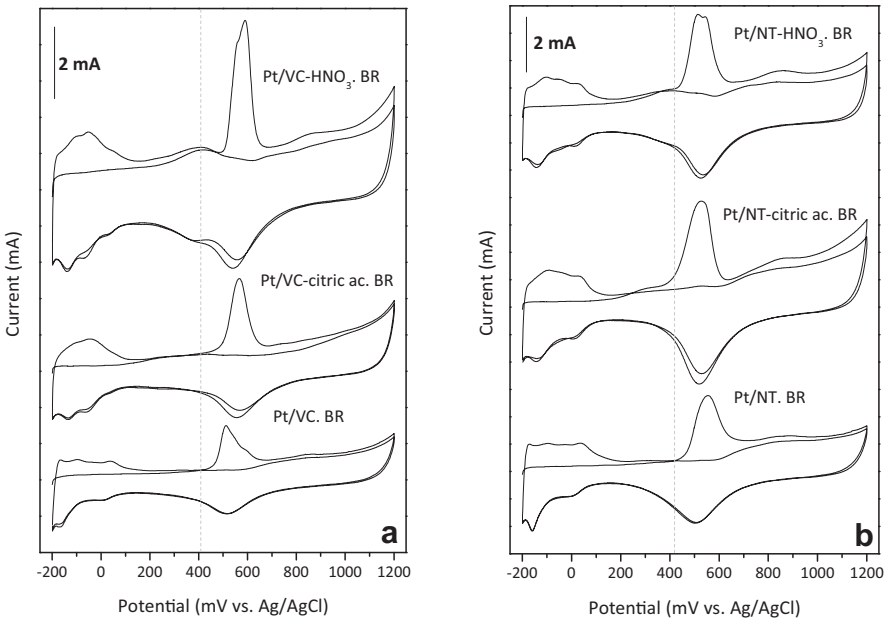

Figure 7. CO stripping of Pt catalysts supported on functionalized and non-functionalized carbons prepared by BR. a) VC and b) NT. Electrolytic solution: H_2SO_4 0.5 M, v = 25 mV/s.

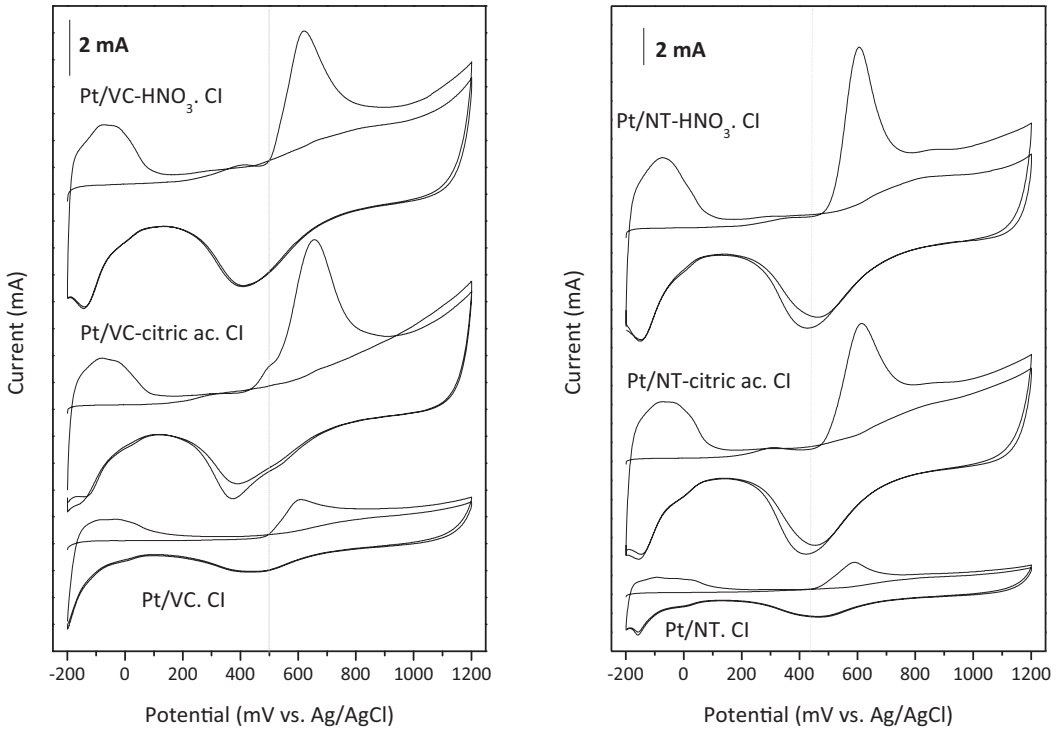

Figure 8. CO stripping of Pt catalysts supported on functionalized and non-functionalized carbons prepared by CI. a) VC and b) NT. Electrolytic solution H_2SO_4 0.5 M, v = 25 mV/s.

Table VI. Onset potential of CO oxidation and EASS values of Pt catalysts supported on functionalized and non-functionalized carbons and prepared by BR.

Catalysts	Onset potential CO oxidation (mV)	EASS (m^2 g Pt^{-1})
Pt/VC. BR	407	12
Pt/VC-citric ac. BR	330	21
Pt/VC-HNO_3. BR	470	31
Pt/NT. BR	419	31
Pt/NT-citric ac. BR	260	38
Pt/NT-HNO_3. BR	364	33

These results agree with the ones published by Stevanovic et al.[48] that postulate that the activity increase of Pt catalysts supported on oxidized supports respect to catalysts over non oxidized ones could be caused by a promoting effect over the CO_{ads} oxidation. The development of functional groups by functionalization treatments with acids could improve the Pt adsorption environment over carbon, thus increasing the interaction between the metal and the modified support, as Yu et al. reported.[49] In consequence, the functional groups developed in the support not only modify the surface chemistry of the carbonaceous material but also the metal-support interaction of the catalyst.

Table VII. Onset potential of CO oxidation and EEAS values of Pt catalysts supported on functionalized and non-functionalized carbons and prepared by CI.

Catalysts	Onset potential CO oxidation (mV)	EASS (m^2 g Pt^{-1})
Pt/VC. CI	500	16
Pt/VC-citric ac. CI	435	88
Pt/VC-HNO_3. CI	480	75
Pt/NT. CI	450	15
Pt/NT-citric ac. CI	450	95
Pt/NT-HNO_3. CI	455	120

Conclusions

The functionalization treatment with nitric acid induces high concentration of strongly acidic functional groups and also weak ones, whereas citric acid promotes the formation of acid groups with an intermediate acidic strength. In this way, oxidized surface groups of different nature are produced by the functionalization treatments with both acids.

The isoelectric points of both supports (Vulcan carbon and carbon nanotubes) decrease after citric acid functionalization, this decrease being more pronounced when functionalized with nitric acid, a stronger oxidant.

By comparing the deposition-reduction method (BR) in liquid phase with the impregnation method (CI), the last one would assure a stronger interaction between the support and the metallic precursor during the impregnation, and lower metallic particle sizes can be attained.

Catalysts prepared by BR and supported on functionalized carbons show a slight modification in the active site-support interaction caused by the functionalization treatment.

For catalysts prepared by CI method and supported on VC, there is a decrease of the mean particle size when the support is functionalized with HNO_3 or citric acid. In this case, the modification of the metal-support interaction would promote the deposition of the metallic precursor in the form of smaller particle sizes. For catalysts prepared by CI and supported on NT, there is also a different interaction between the metal and the functionalized carbon.

Finally, catalysts prepared by CI and supported on functionalized VC and NT display much higher electrochemical active areas than those supported on the corresponding non-functionalized carbons. Both the decrease of the metallic particle sizes and the changes in the

metal-support interaction due to the presence of the functional groups of the carbons would lead to better electrochemical behaviors.

Acknowledgments

Authors thank to Julieta Vilella for her assistance. This work was made with the financial support of Universidad Nacional del Litoral and CONICET.

References

1. S. Sharma and B. G. Pollet, *J. Power Sources*, **208**, 96 (2012).
2. S. F. Yin, B. Q. Xu, X. P. Zhou, and C. T. Au, *Appl. Catal. A*, **277**, 1 (2004).
3. M. de Becdelievre, J. de Becdelievre, and J. Clavilier, *J. Electroanal. Chem.*, **294**, 97 (1990).
4. B. Beden, C. Lamy, N. R. de Tacconi, and A. J. Arvia, *Electrochim. Acta*, **35**, 691 (1990).
5. V. E. Kazarinov, V. N. Andreev, and A. V. Shlepakov, *Electrochim. Acta*, **34**, 905 (1989).
6. G. Hoogers and D. Thompsett, *Cattech*., **3**, 106 (2000).
7. H. B. Zhang, G. D. Lin, Z. H. Zhou, X. Dong, and T. Chen, *Carbon*, **40**, 2429 (2002).
8. E. M. Crabb and M. K. Ravikumar, *Electrochim. Acta*, **46**, 1033 (2001).
9. J. R. C. Salgado, V. A. Paganin, E. R. Gonzalez, M. F. Montemor, I. Tacchini, A. Ansón, M. A. Salvador, P. Ferreira, F. M. L. Figueiredo, and M. G. S. Ferreira, *Int. J. Hydrogen Energy*, **38**, 910 (2013).
10. L. Calvillo, M. J. Lázaro, I. Suelves, Y. Echegoyen, E. G. Bordejé, and R. Moliner, *J. Nanosci. Nanotechno.*, **9**, 4164 (2009).
11. T. G. Ros, A. J. van Dillen, J. W. Geus, and D. C. Koningsberger, *Chem-Eur. J.*, **8**, 1151 (2002).
12. M. L. Toebes, J. M. P. van Heeswijk, J. H. Bitter, A. J. van Dillen, and K. P. de Jong, *Carbon*, **42**, 307 (2004).
13. A. Guha, W. Lu, A. Zawodzinski, and D. A. Schiraldi, *Carbon*, **45**, 1506 (2007).
14. J. Guo, G. Sun, Q. Wang, G. Wang, Z. Zhou, S. Tang, L. Jiang, B. Zhou, and Q. Xin, *Carbon*, **44**, 152 (2006).
15. F. Zaragoza-Martín, D. Sopeña-Escario, E. Murallón, and C. Salinas-Martínez de Lecea, *J. Power Sources*, **171**, 302 (2007).
16. X. Yu and S. Ye, *J. Power Sources*, **172**, 133 (2007).
17. S. J. Park, J. M. Park, and M. K. Seo, *J. Colloid Interface Sci.*, **337**, 300 (2009).
18. S. S. Barton, M. J. B. Evans, and E. Halliop, *Carbon*, **35**, 1361 (1997).
19. L. Figueiredo, M. F. R. Pereira, M. M. A. Freitas, and J. J. M. Orfao, *Carbon*, **37**, 1379 (1999).
20. H. P. Boehm, *Carbon*, **40**, 145 (2002).
21. M. A. Fraga, E. Jordao, M. M. A. Freitas, J. L. Faria, and J. L. Figueiredo, *J. Catal.*, **209**, 355 (2002).
22. G. C. Torres, E. L. Jablonski, G. T. Baronetti, A. A. Castro, S. R. de Miguel, O. A. Scelza, D. M. Blanco, M. A. Peña Jimenez, and J. L. G. Fierro, *Appl. Catal. A Gen.*,**161**,213 (1997).
23. I. M. J. Vilella, S. R. de Miguel, C. Salinas-Martínez de Lecea, A. Linares-Solano, and O. A. Scelza, *Appl. Catal. A Gen.*, **281**, 247 (2005).
24. C. K. Poh, S. H. Lim, H. Pan, J. Lin, and J. Y. Lee, *J. Power Sources*, **176**, 70 (2008).
25. SEM JOEL-JMS-35C USER GUIDE.
26. M. A. Álvarez-Merino, M. A. Fontecha-Cámara, V. López-Ramón, and C. Moreno-Castilla, *Carbon*, **46**, 778 (2008).
27. J. P. Brunelle, *Pure Appl. Chem.*, **50**, 1211 (1978).
28. N. Veizaga, J. Fernandez, M. Bruno, O. Scelza, and S. de Miguel, *Int. J. Hydrogen Energy*, **37**, 17910 (2012).
29. F. Maillard, M. Eikerling, O. V. Cherstiouk, S. Schreier, E. Savinova, and U. Stimming, *Faraday Discuss*, **125**, 357 (2004).
30. I. M. J. Vilella, *Doctoral thesis*. Santa Fe- Argentina: UNL; 2002.
31. A. Solhy, B. F. Machado, J. Beausoleil, Y. Kihn, F. Goncalves, M. F. R. Pereira, J. J. M. Orfão, J. L. Figueiredo, J. L. Faria, and P. Serp, *Carbon*, **46**, 1194 (2008).
32. E. Aksoylu, M. Madalena, A. Freitas, M. Fernando, R. Perera, and J. L. Figueiredo, *Carbon*, **39**, 175 (2001).
33. J. L. Gómez de la Fuente, S. Rojas, M. V. Martinez-Huerta, P. Terreros, M. A. Peña, and J. L. G. Fierro, *Carbon*, **44**, 1919 (2006).
34. F. Coloma, A. Sepúlveda-Escribano, J. L. G. Fierro, and F. Rodríguez-Reinoso, *Langmuir*, **10**, 750 (1994).
35. P. D. Zgolicz, J. P. Stassi, M. J. Yañez, O. A. Scelza, and S. R. de Miguel, *J. Catal.*, **290**, 37 (2012).
36. M. C. Román-Martınez, D. Cazorla-Amorós, A. Linares-Solano, C. Salinas-Martínez de Lecea, H. Yamashita, and M. Ampo, *Carbon*, **33**, 3 (1995)
37. S. R. de Miguel, M. C. Román-Martınez, E. Jablonski, J. L. G. Fierro, D. Cazorla-Amorós, and O. A. Scelza, *J. Catal.*, **184**, 514 (1999).
38. A. Sepulveda-Escribano, F. Coloma, and F. Rodriguez-Reinoso, *Appl. Catal. A*, **173**, 247 (1998).
39. E. Antolini, *Appl. Catal. B Environ.*, **88**, 1 (2009).
40. M. C. Roman-Martinez, D. Cazorla-Amoros, A. Linares-Solano, and C. Salinas-Martinez de Lecea, *Carbon*, **31**, 895 (1993).
41. M. H. Treptau and D. J. Miller, *Carbon*, **29**, 531 (1991).
42. J. M. Calo, D. Cazorla-Amoros, A. Linares-Solano, M. C. Roman-Martinez, and C. Salinas-Martinez de Lecea, *Carbon*, **35**, 543 (1997).
43. N. Mahata, F. Goncalves, M. F. R. Pereira, and J. L. Figueiredo, *Appl. Catal. A Gen.*, **339**, 159 (2008).
44. B. da Silva, E. Jordäo, M. J. Mendes, and P. Fouilloux, *Appl. Catal. A Gen.*, **148**, 253 (1997).
45. D. Poondi and M. A. Vannice, *J. Catal.*, **161**, 742 (1996).
46. G. Haller, *J. Catal.*, **216**, 12 (2003).
47. B. Zhong, H. Liu, X. Gu, and D. S. Su, *ChemCatChem*, **6**, 1553 (2014).
48. S. Stevanovic, V. Panic, D. Tripkovic, and V. M. Javanovic, *Electrochem. Commun.*, **11**, 18 (2009).
49. R. Yu, L. Chen, Q. Liu, J. Lin, K. L. Tan, S. C. Ng, H. S. O. Chan, G. Q. Xu, and T. S. A. Hor, *Chem. Mater.*, **10**, 718 (1998).